

Anti-Reflection Strategies for Sub-0.18- μm Dual Damascene Structure Patterning in KrF 248nm Lithography

Shuo-Yen Chou^a, Chien-Ming Wang^b, Chin-Chiu Hsia^b, Li-Jui Chen^b, Gue-Wuu Hwang^b,
Shyh-Dar Lee^b, and Jen-Chung Lou^a

^aInstitute of Electronics, National Chiao Tung University, Hsinchu, 300, Taiwan, R. O. C.

^bDeep Sub-micron Division, ERSO, ITRI, Chutung, Hsinchu, 310, Taiwan, R. O. C.

ABSTRACT

Finding high performance and low cost anti-reflection strategies is a common goal for all photolithographers. This task is getting tough for dual damascene process than the metal-etch process because the oxide thickness variation enhances the thin film interference effect. In this paper, different ARC strategies using organic and inorganic material were examined to compare their CD control performance in sub-0.18 μm dual damascene structure for KrF 248nm lithography. The organic bottom ARC (BARC) achieves reflectivity control through modulating its thickness. The first and second minimal points in BARC swing curve were chosen as the film thickness to be evaluated. The inorganic ARC, which referred to dielectric ARC (DARC) using PECVD silicon oxynitride (SiO_xN_y) in this article, was investigated with single layer and double layer structures. The double-layer DARC structure consists of two layers with different extinction coefficient K values. The optimal refractive index (N , K) and thickness of each ARC structure were calculated from some available photolithography simulators. A PECVD process for DARC growth that provides easily tunable range of refractive index and thickness was established to meet the DUV process requirement from simulation. The performances of each ARC structure were evaluated on patterning 0.18 μm trench and 0.20 μm via in back-end-of-line (BEOL) dual damascene process. It showed that the double-layer DARC provided the most effective CD control ability among these ARC structures. The double-layer DARC should be one of the most potential candidates for sub-0.18 μm dual damascene process.

Keywords: DUV lithography, sub-0.18 micron, KrF, Thin Film Interference, reflectivity control, CD control, BARC, DARC, SiON, dual damascene

1. INTRODUCTION

Lithographic patterning for finer critical dimension (CD) was imminently demanded as the IC design rule continues to shrink for the purpose of increasing circuit packing density and accelerating device speed. The stepper systems with higher NA lens and shorter exposure wavelength from near UV to deep UV were used to enhance resolution according to Rayleigh criterion. The KrF 248nm excimer laser lithography was capable to print sub-0.18 μm geometry with the aid of off-axis illumination (OAI)[1] and phase-shifting mask (PSM). Since the CD budget gets small and process window (energy latitude, depth of focus) shrinks as CD miniaturized, stringent CD control must be achieved for sufficient production capability. Swing effect, which comes from the absorption energy fluctuation in resist, is a main contributor to CD variation. To minimize this effect, the most realistic method is applying the anti-reflective coating (ARC) to eliminate the substrate reflectivity in resist.

For the conventional subtractive process used to fabricate aluminum interconnects, the purpose of ARC layer was to minimize the scattering light from topography or grainy surface of metal. Since the optical condition of metal substrate doesn't change with the thickness variation of metal layer, a conformal ARC layer performed perfect destructive interference would be acceptable. Dual damascene process, an alternative interconnect technology, becomes prevailing in semiconductor manufacturing as the development of copper interconnect technology. Such process replaces the metal-etch as critical step to define the width and spacing of lines by a simpler dielectric-etch. Since lithography of dual damascene process is done upon the dielectric rather than metal layer, thin film interference is another issue the anti-reflection strategy must handle. Thin film interference comes from the monochromic exposure wavelength and a multilayer medium composed of transparent interlayer dielectric and a highly reflective substrate. The interlayer dielectric, such as nitride, USG, BPSG, FSG etc., is often transparent with extinction coefficient of zero at 248nm wavelength. Since most of these materials are silicon dioxide based. We abbreviated the transparent dielectric as oxide in this article. The zero extinction coefficient makes the light pass through the oxide layer without losing intensity, but its phase varies as it goes through the oxide layer because of the real part of refractive index. The light reflects back from the reflective substrate. Part of the light will reflect

back into the oxide again and part will transport into the resist and interfere with reflective light from resist /oxide interface. The light reflects back and forth in the oxide layer and causes energy fluctuation in the resist as oxide thickness variation. The thin film interference gets worse as the exposure wavelength becomes shorter. Since shorter wavelength shrinks the period of swing curve that is dominated by equation $\lambda/4n_{oxide}$, therefore, it results in smaller latitude of thickness variation. Such precision control of dielectric thickness can't be actualized from state-of-the-art thin film deposition or planarization techniques, let alone there are innate thickness difference from crossing topography.

In this paper, different ARC strategies using organic and inorganic materials were examined to compare their CD control performance in 0.18 μ m trench and 0.2 μ m via patterning for KrF 248nm lithography. The organic bottom ARC (BARC) achieves reflectivity control through modulating its thickness. The first and second minimal points in BARC swing curve were chosen as the film thickness to be evaluated. The inorganic ARC, which referred to dielectric ARC (DARC) using silicon oxynitride (SiO_xN_y) in this article, was investigated with single layer and double layer structures. A PECVD process for DARC growth that provided easily tunable range of refractive index was established to meet the DUV process requirement from simulation.

2. SIMULATION BACKGROUND AND EXPERIMENTAL CONDITION

1. Theoretical Background

In this section, we briefly describe the theoretical background of simulation to find the optimal optical condition of each ARC strategy. Consider the case when an electromagnetic radiation strikes the surface of an absorbing material medium such as BARC. Let $n_2=N_2-iK_2$ the index of refraction of absorbing medium and $n_1=N_1$ be the index of the incident medium (photoresist, neglect the small extinction coefficient). A direct application of the Snell law leads to

$$N_1 \sin \theta_1 = (N_2 - iK_2) \sin \theta_2$$

where θ_1 is the angle of incident and θ_2 is the angle of refraction. According to Maxwell's equations, the reflection coefficient of a plane wave at a plane interface between two media with semi-infinite thickness is obtained as the form of

$$r_s = \frac{k_{1x} - k_{2x}}{k_{1x} + k_{2x}} \dots (1) \quad r_p = \frac{N_1^2 k_{2x} - N_2^2 k_{1x}}{N_1^2 k_{2x} + N_2^2 k_{1x}} \dots (2)$$

where k_{1x} and k_{2x} are the normal components of the wave vectors in medium 1 and 2, which can be written as

$$k_{1x} = \left[\left(\frac{\omega}{c} N_1 \right)^2 - \left(\frac{\omega}{c} \sin \theta_1 \right)^2 \right]^{1/2} \dots (3) \quad \text{and} \quad k_{2x} = \left[\left(\frac{\omega}{c} \right)^2 (N_2 - iK_2)^2 - \left(\frac{\omega}{c} \sin \theta_1 \right)^2 \right]^{1/2} \dots (4)$$

When high NA lens and OAI illumination were used, the zero order light will have an oblique angle of incident. But since this effect in our 0.55NA lens was too small to produce significant simulation error, we only consider the vertical propagation case with $\theta_1 = \theta_2 = 0$. The Fresnel reflection coefficients becomes

$$r_s = r_p = \frac{N_1 - (N_2 - iK_2)}{N_1 + (N_2 - iK_2)} \dots (5)$$

The reflectivity at normal incident is thus

$$R = |r_s|^2 = |r_p|^2 = \frac{(N_1 - N_2)^2 + K_2^2}{(N_1 + N_2)^2 + K_2^2} \dots (6)$$

Equation (4) isn't the final formula used to calculate the reflectivity of stack films, but it can provide a qualitative measurement of how much intrinsic reflectivity will be due to index of refractive mismatch of two media.

In reality, lithography was often done upon substrate with multilayer stacking. When the number of layers becomes large, it's better to calculate the reflection of electromagnetic radiation using 2 \times 2-matrix method[2]. Applying the method and using the assumption of normal incident, the characteristic matrix of a multilayer medium is given by

$$D_l = \begin{pmatrix} 1 & 1 \\ n_l & -n_l \end{pmatrix} \dots (7) \quad \text{and} \quad P_l = \begin{pmatrix} e^{i\phi_l} & 0 \\ 0 & e^{-i\phi_l} \end{pmatrix} \dots (8)$$

where

$$\begin{pmatrix} M_{11} & M_{12} \\ M_{21} & M_{22} \end{pmatrix} = D_0^{-1} \left[\prod_{l=1}^N D_l P_l D_l^{-1} \right] D_s \dots (6)$$

with

$$\phi_l = k_{lx}d_l$$

Suffix 0 denotes the incident medium, suffix l denotes the l th layer from incident medium, and suffix s denotes the substrate. The l th layer thickness was denoted by d_l .

Reflectivity from a multilayer medium is given by

$$R = |r|^2 = \left| \frac{M_{21}}{M_{11}} \right|^2 \dots (9)$$

Equation (9) was applied to our computer program to calculate the reflectivity of a multilayer medium and identify the optimal optical conditions for ARC layer coating.

2. Experimental Conditions

200mm wafers were used in these studies. The experimental samples were bare silicon wafers with the addition of undoped silicon glass (USG) deposited. The organic BARC was applied by spin coating and then curing. The silicon oxynitride (SiO_xN_y) played as DARC was prepared by PECVD system with 6 sequel chambers, which can enhance the throughput. The SiON film was formed using $\text{SiH}_4/\text{N}_2\text{O}$ chemistry. The thickness and refractive index of each film were determined using spectroscopic ellipsometer[3]. The refractive index of each material extracted by spectroscopic ellipsometer was listed in Table 1.

A KrF excimer laser stepper with 0.55 NA lens was used to expose the wafers. Annular 1/2 illumination and HTSPM with 6% transmittance were applied to improve resolution. The CD swing of oxide thickness variation and resist thickness variation with different ARC strategies was characterized by 0.18 μm trench and 0.2 μm via. All CD measurement was done by top-down CD-SEM.

	Silicon	USG	BARC	Photoresist
Real part of refractive index: N	1.570	1.523	1.445	1.76
Extinction coefficient: K	3.564	0	0.409	0.010

Table 1. Refractive index of thin film using in simulation

3. RESULT AND DISCUSSION

1. BARC approach

Fig. 1 shows how the spin-coated BARC handles the reflectivity in resist. Referred to Fig. 1(a), as the BARC thickness changes from zero to about 0.1 μm , the reflectivity varies drastically because the anti-reflection ability were mainly come from phase cancellation in this range of thickness. The fluctuation will be damped as BARC thickness increasing. When the thickness is more than 0.2 μm , the swing is almost diminished and only the intrinsic reflectivity due to the mismatch of optical constants of resist and oxide exists. From Fig. 1(b), the BARC thickness that reach first minimums with substrate reflectivity less than 2% was 450 \AA for oxide thickness of 0.83 μm , 760 \AA for 0.80 μm , and 1050 \AA for 0.83 μm , respectively. Taking these data as parameters of BARC thickness and calculating the reflectivity in resist as a function of oxide thickness, we found pronounce swing characteristic as shown in Fig. 1(c). The worst case happened at the condition of 450 \AA BARC coating, because small amount of deviation from the optimal oxide thickness would cause the reflectivity exceeding than 5%. The case of BARC with thickness about 1000 \AA performed the best result because reflectivity in resist was controlled within 6% no matter how much the oxide thickness deviated. Is a reflectivity control within 6% enough for 0.18 μm or even sub-0.18 μm structure patterning? Base on our experimental work, the answer is no. As indicated in Fig. 2(a), more than half of the CD budget (18nm/36nm) of 0.18 μm trench pattern was consumed by 400 \AA oxide thickness variation when BARC with 1K \AA thickness was applied. Therefore, ARC strategy with first reflectivity minimum as BARC thickness is not a proper choice for sub-0.18 μm structure patterning since control substrate reflectivity to be within 6% is not enough to reduce CD swing.

BARC layers with thickness of first minimum substrate reflectivity failed due to lack of absorption. The mechanism of anti-reflections depends on phase cancellation because of the small extinction coefficient K and thin thickness of the BARC. When the absorption is weak in BARC layer, the light transmitted through the BARC will finally be reflected off from the substrate without losing significant intensity, but its phase will vary acutely as long as there is little difference in optical path from transparent layers. To avoid this phenomenon, the thickness of BARC must be further increased to provide more absorption. Accordingly, it's better to choose the second minimum points indicated in Fig. 1(a) as the layer thickness of BARC. Fig. 1(d) shows the reflectivity swing curves as a function of oxide thickness corresponding to BARC thickness of 1270 \AA , 1600 \AA , and 2000 \AA , respectively. The CD swing of BARC 1.6K \AA was about half of that from BARC 1K \AA as shown in Fig. 2(b). When the BARC thickness reached 2K \AA , the swing effect diminished, referred to Fig. 2(c).

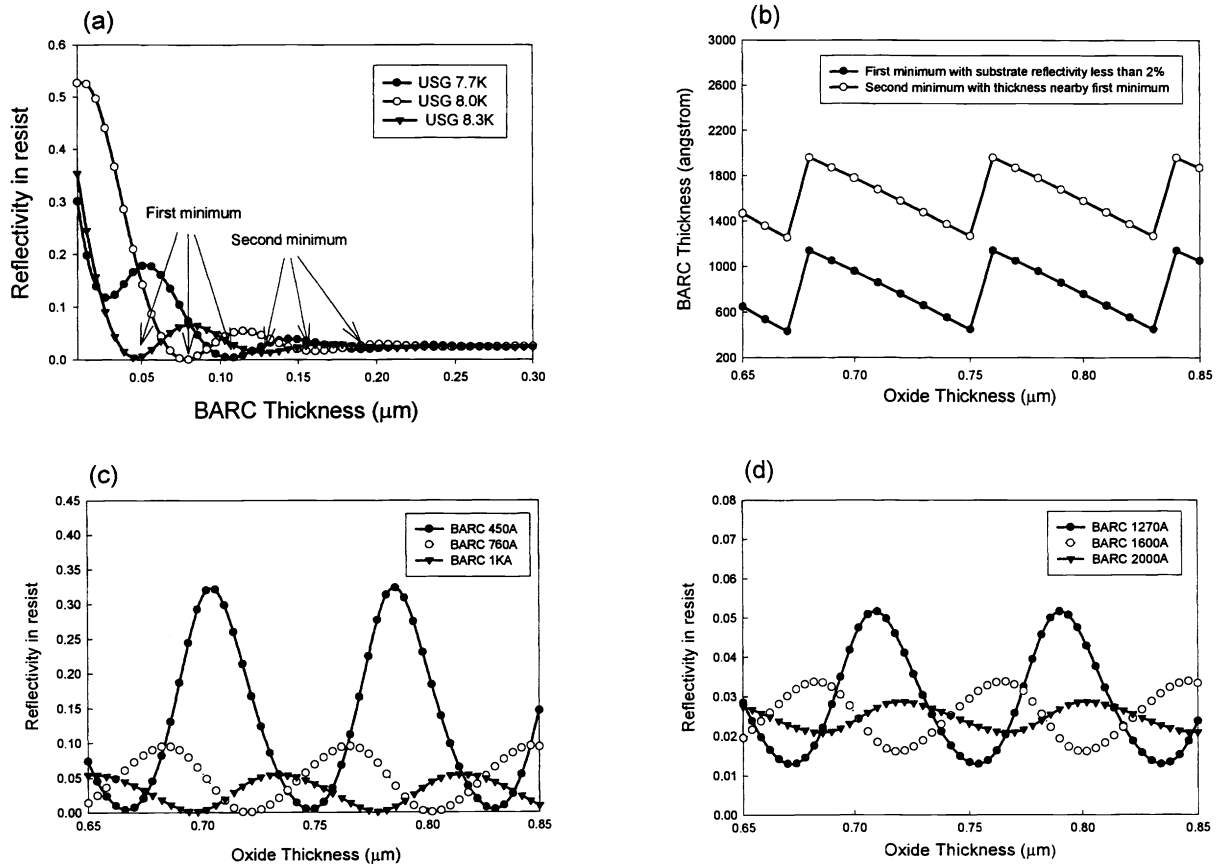


Fig.1 (a) Reflectivity in resist vs. thickness of BARC with oxide thickness varies from $0.77\mu\text{m}$ to $0.83\mu\text{m}$. (b) First minimum and second minimum position of BARC thickness vs. oxide thickness. (c) Reflectivity in resist vs. thickness of oxide at first minimums of BARC thickness. (d) Reflectivity in resist vs. thickness of oxide at second minimums of BARC thickness.

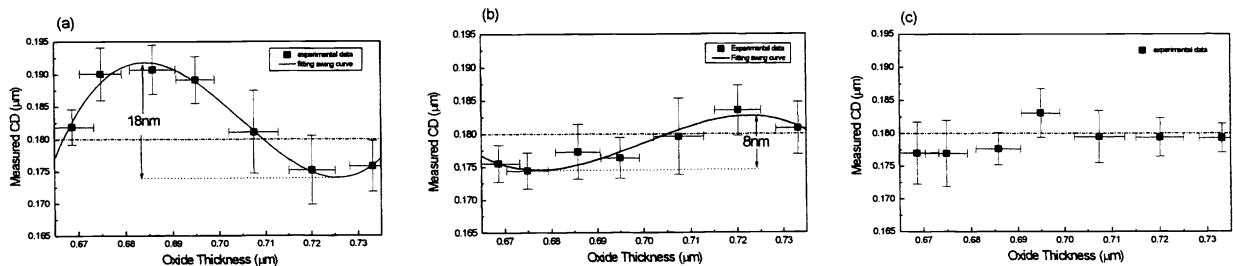


Fig. 2 Oxide thickness vs. critical dimension for $0.18\mu\text{m}$ trench pattern with (a) $1\text{K}\text{\AA}$ BARC coating, (b) $1.6\text{K}\text{\AA}$ BARC coating, and (c) $2\text{K}\text{\AA}$ BARC coating. 3-sigma error bar was also added in these figures.

It seems that the BARC with thickness located at the second minimums of the reflectivity curves are better choice than that at the first minimums to overcome the oxide thickness variation, but there are disadvantages of the application of thick BARC. As the critical dimension shrinks, the resist thickness was decreased because of the constraint of aspect ratio of geometry and for the purpose of depth of focus and resolution enhancement. Because of the small etch selectivity between BARC and photoresist, thicker BARC means more photoresist loss during the breakthrough of BARC and the resistance to etchant suffers. It will lead to the degradation of etching process control. Besides, negative CD bias (wafer CD minus mask

CD is equal to CD bias) should be taken because the breakthrough process of BARC etching would enlarge CD. Negative CD bias implies smaller target CD in lithography, thus results in smaller exposure latitude and depth of focus. As a result, there is a trade-off between lithography and etching process when BARC approach was utilized in dual damascene process. One way to solve the dilemma was to increase the optical density of the BARC in order to dampen the swing in thinner thickness. But researchers found that the etching resistance of commercial available BARC would hike as its optical density increases[4-5].

The third problem for the application of thick BARC is the insufficient CD swing control ability due to photoresist thickness variation. Because of the mismatch between the optical constants of resist and BARC, no matter how thick the BARC applies, it always poses an intrinsic reflectivity at the interface of resist and BARC. From Fig. 1(a) and 1(d), the residual reflectivity of BARC with thickness over second minimums is about 2.5%. Such small amount of substrate reflectivity is enough to cause serious interference in the air/resist interface as indicated in Fig. 3. Because the reflectivity is represented in intensity, which is the square of the amplitude, even 1% substrate reflectivity would result in 10% magnitude of the amplitude of reflected light. Fig. 4(a) and Fig. 4(b) show the CD swing curve of 0.18 μm trench and 0.2 μm via respectively. From these experimental data, the CD variation due to resist thickness variation consumed almost two third of the CD budget even with a BARC layer of 0.2- μm thickness. The CD swing problem due to resist thickness variation would be much alleviated in dual damascene process when the dielectric surface is planarized by CMP process as well as the use of conformal photoresist.

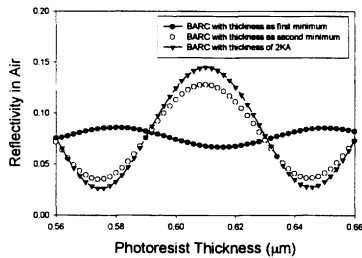


Fig. 3 Reflectivity in air vs. resist thickness with different BARC thickness and 0.82 μm oxide thickness

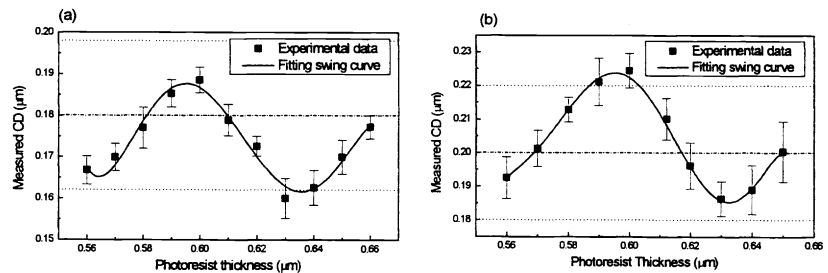


Fig. 4 Photoresist thickness vs. critical dimension with 2KÅ BARC coating for (a) 0.18 μm trench pattern and (b) 0.20 μm via pattern. 3-sigma error bar was also added.

2. DARC Approach

The DARC, which referred to silicon oxynitride in this article, is a promising candidate as anti-reflective layer because of its optical tunability, cost and production control [6-8]. The optimal combination of optical constants (N and K) and thickness for DARC were calculated using the theorem described in section 2.1. The result for testing structure is presented in the form of a contour plot of the substrate reflectivity, as shown in Fig. 5. The substrate reflectivity of such multilayer structure will be annihilated when the DARC inhibits a combination of optical constants with $N=1.98$, $K=0.605$, and $T=60\text{nm}$. Fig. 6 shows the substrate reflectivity as functions of oxide thickness and DARC thickness. This combination of optical constants is insufficient to overcome the oxide thickness variation because the mechanism of anti-reflection mainly depends on destructive interference.

Compared with the substrate reflectivity in resist of BARC and DARC (reference to Fig. 8), the swing ratio of DARC is comparable with BARC whose thickness located at first minimums of reflectivity, therefore, the DARC designed by conventional conception of phase cancellation is unable to suppress the CD swing. To get effective CD control regardless of the oxide thickness variation, a novel design of DARC must be applied for dual damascene structure patterning.

According to the result of BARC, the most effective method to get rid of CD swing form oxide thickness variation is to enhance the absorption ability of the ARC layer either by raising the extinction coefficient K or increasing the layer thickness. The extinction coefficient of SiON could be raised to as high as 1.3, but according to the Fresnel reflection formulas (Equation (6) of section 2), such high extinction coefficient inversely increases the reflectivity because the large difference between the optical constants of resist and ARC. Increasing the thickness of the DARC to improve absorption ability is infeasible by reason that the process window of SiON with tunable N and K only ranges from about 200Å to 500Å thickness. Accordingly, the strategy to design the DARC on oxide layers must be different from that of BARC, which is merely increasing the thickness.

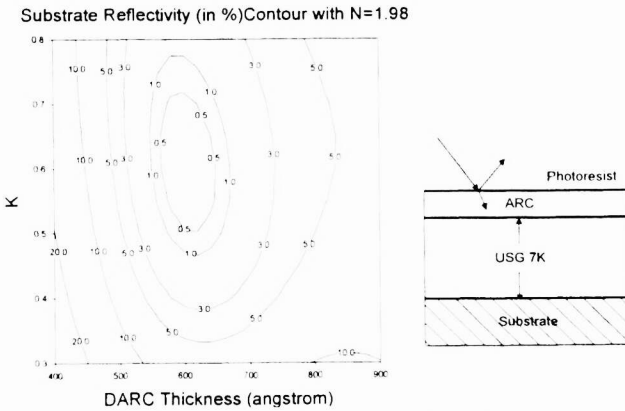


Fig. 5 Contour plot of substrate reflectivity in resist with real part of refractive index $N=1.98$

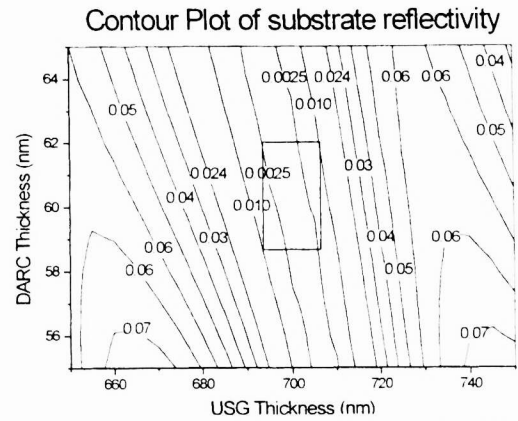


Fig. 6 Contour plot of substrate reflectivity in resist with $N=1.98$, $K=0.605$, and $T=60\text{nm}$

A novel DARC design is applied here to take over the conventional destructive-mode design[9]. The scheme of the double-layer DARC design is illustrated in Fig. 7(a). First, a SiON layer with high extinction coefficient and moderate thickness (around 300\AA) is deposited on substrate stack. The main purpose of such layer is not only to increase the absorption of incident light but also to isolate the optical characteristics of film stacks, especially for the transparent dielectric layers. The following process is another SiON layer deposition. The optical constants of the second SiON layer is designed based on the mechanism of phase cancellation with the real part of refractive index the same as first SiON layer, hence it can completely annihilate the substrate reflectivity without any residual background reflectivity. Fig. 7(b) shows the simulation result for the optimization of optical constants of second SiON layer. Compared with Fig. 5, the double-layer DARC have wider process window of reflectivity within 1% than single layer structure. What will happen if substrate oxide thickness varies? Since the first SiON layer strongly modulated the optical condition of the substrate stacks, the deviation of oxide thickness will do little to alter the substrate reflectivity because the optical characteristic of substrate was mostly decided by the first SiON layer (Bottom DARC layer). Since the optical condition of substrate including bottom DARC doesn't change very much as underneath oxide thickness varying, the anti-reflective ability of top DARC (second SiON layer) due to destructive interference would not suffer too much from oxide thickness variation. It's worth noting that both top DARC and bottom DARC in our design have the same real part of refractive index, N , which is about 2. Two benefits come from this process requirement. First, the same real part of refractive index (N) reduces the reflection between top DARC and bottom DARC layer. Such small amount of reflective light source from the interface of two DARC layers would be further decreased as it goes through top DARC with somewhat absorption ability. Therefore, the top DARC gets more immunity from variation of substrate condition. The second advantage is the refractive index of SiON is closer to DUV resist (about 1.8) than commercial DUV organic ARC (about 1.45). Therefore, smaller intrinsic reflectivity occurred at the resist/ARC interface. It could improve the CD swing control as resist thickness variation. The comparison of reflectivity control among different ARC strategies is presented in Fig. 8. The double-layer DARC behaved as the best choice to overcome oxide thickness variation. Fig. 9 and Fig. 10 indicate the excellent CD control ability of double-layer DARC as substrate oxide thickness and photoresist thickness vary.

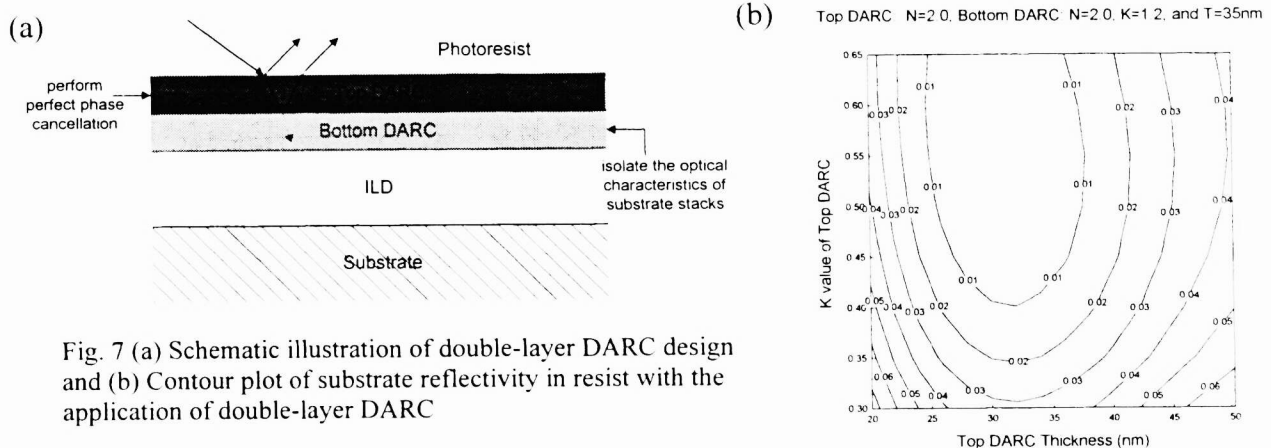


Fig. 7 (a) Schematic illustration of double-layer DARC design and (b) Contour plot of substrate reflectivity in resist with the application of double-layer DARC

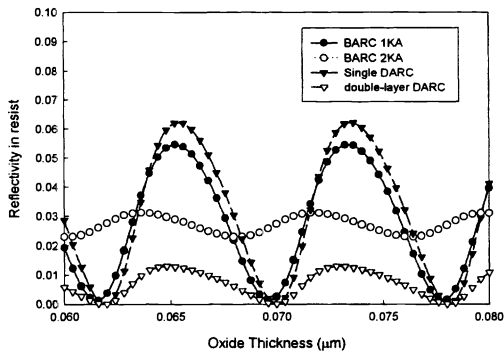


Fig. 8 Comparison of the substrate reflectivity control between different ARC strategies

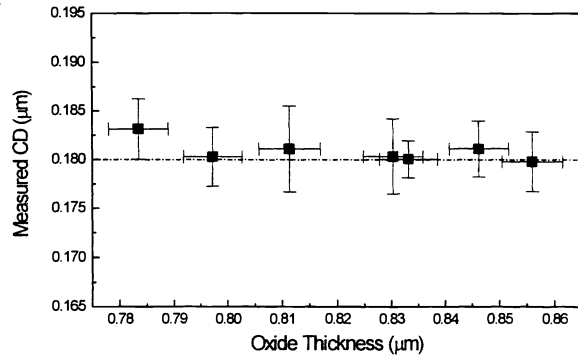


Fig. 9 Oxide thickness vs. critical dimension of $0.18\mu\text{m}$ trench with the application of double-layer DARC. 3-sigma error bar was also added.

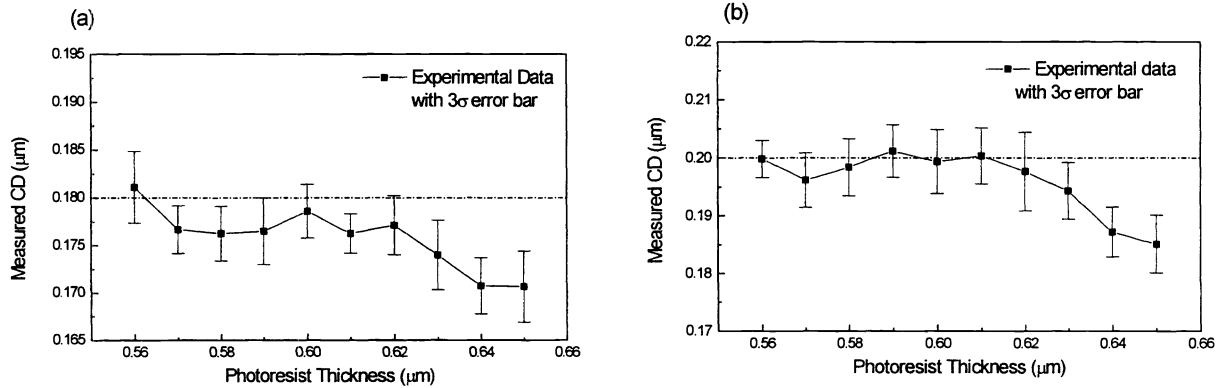


Fig. 10 Photoresist thickness vs. critical dimension of (a) $0.18\mu\text{m}$ trench and (b) $0.20\mu\text{m}$ via with the application of double-layer DARC. No swing effect but bulk effect was observed in these figures.

3. CD uniformity testing for BARC and double-layer DARC approach

For CD uniformity testing, five silicon wafers with about $0.825\mu\text{m}$ USG layers deposited were taken as experimental samples. The wafer condition is listed in Table I. The CD target is $0.18\mu\text{m}$ trench pattern. 180 measurements were made in each wafer. Table 2 lists the USG thickness uniformity of each wafer. Table 3 lists the CD uniformity result.

From Table 2, the thickness difference within a single wafer is about 110\AA and the maximum thickness variation among these five wafers is 250\AA . Such small variation would be enough to make significant impact on CD uniformity when different anti-reflection strategies were applied, as shown in Table 3 and Fig. 11. When BARC layers with thickness of 570\AA are used, the within wafer CD uniformity and crossing wafer CD uniformity are both bad due to the poor reflection control stability of phase cancellation mechanism. The within wafer CD uniformity is good for $1\text{k}\text{\AA}$ BARC because the reflectivity swing is moderated within such small amount of 110\AA thickness variation. But the wafer to wafer CD uniformity of $1\text{k}\text{\AA}$ BARC is slightly degraded because the CD swing effect causes the average CD value of each wafer varying as indicated in Fig. 2(a). The BARC $2\text{k}\text{\AA}$ approach and double-layer DARC approach performed excellently within wafer and crossing wafer CD uniformity. The CD swing problem of resist thickness variation for BARC $2\text{k}\text{\AA}$ approach doesn't appeal since the testing wafers have planar surface and the spin-coated resist is conformal. Fig. 11 shows the histograms of crossing-wafer CD measurement when different ARC strategies applied.

49 points thickness measurement with 6mm edge exclusion (unit: angstrom)					
Wafer ID.	1	2	3	4	5
Max.	8359.0	8328.2	8295.2	8288.0	8269.7
Min.	8210.2	8174.7	8136.5	8128.4	8114.9
Average	8290.5	8257.2	8218.4	8209.6	8195.8
3 sigma	105.3	108.3	112.4	110.7	110.2

Table 2. Wafer condition for CD uniformity testing

		Within wafer inter-field uniformity (unit: nm)					WTW uniformity (unit: nm)
		Wafer 1	Wafer 2	Wafer 3	Wafer 4	Wafer 5	
BARC 570Å	Mean	179.6	167.7	174.1	183.7	177.8	176.7
	3 Sigma	11.9	17.1	18.3	16.7	15.4	22.7
BARC 1KÅ	Mean	186.3	184.7	180.8	180.7	181.5	182.8
	3 Sigma	9.0	7.2	6.9	7.2	6.4	10.0
BARC 2KÅ	Mean	179.9	178.6	181.3	181.9	181.5	181.0
	3 Sigma	7.3	7.1	6.2	8	7.2	8.6
Double-layer DARC	Mean	179.1	178.4	179.8	181.9	179.5	179.7
	3 Sigma	6.3	5.9	6.8	6.9	7.5	7.6

Table 3 Statistic results of CD uniformity for different ARC strategies

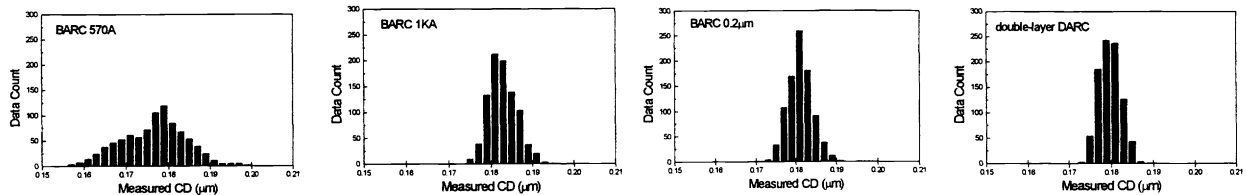


Fig. 11 Histogram of crossing-wafer measurement for different ARC strategies

4. CONCLUSION

In order to reduce the swing effect due to thin film interference from the dielectric thickness variation, effective ARC strategies must be applied in dual damascene structure patterning. The ARC strategy using BARC with thickness located at first minimums was disqualified since the anti-reflective ability degrades drastically when the optical condition of substrate, such as layer thickness, changes. The commercial available BARC can achieve good resist CD control by merely increasing the thickness over the second minimum points of reflectivity. But the after-etch CD control would be a challenge because thicker BARC means more photoresist loss in etching process. Another shortcoming is the CD swing as resist thickness variation due to the mismatch of optical constants between resist and BARC.

The conventional design of the DARC is not suitable for dual damascene structure patterning because of its poor reflectivity control over the transparent oxide layer. A new double-layer DARC design is applied in this article to conquer the oxide thickness variation. For the double-layer DARC process, a thin silicon oxynitride layer was first deposited with high extinction coefficient in order to isolate the transparent characteristic of substrate stacks, and followed the deposition of second oxynitride layer with optical constants optimized to perform perfect destructive interference. A nearly zero CD swing is shown in our experimental data independent of oxide thickness variation or resist thickness variation. Excellent CD uniformity of 0.18µm trench was achieved via the double-layer DARC approach. Compared with BARC and single DARC approach, the double-layer DARC approach is the most promising one to be applied in sub-0.18µm dual damascene structure patterning.

5. ACKNOWLEDGEMENTS

The authors would like to thank Dr. Chien-Mei Wang and Dr. Wen-Dyi Lin for their supporting to prepare experimental samples.

6. REFERENCES

1. C. C. Hsia, T. S. Gau, C. H. Yang, R. G. Liu, C. H. Chang, L. J. Chen, C. M. Wang, G. W. Hwang, J. W. Lay, D. Y. Goang, "Customized off-axis illumination aperture filtering for sub-0.18- μm KrF lithography", to be published in Proc. SPIE's 24th Symp. On Microlithography, 1999.
2. P. Yeh, "Optical Waves in Layered Media", chapter 5, John Wiley & Sons, 1991
3. C. Defranoux, J.P. Piel, J.L. Stehle, "Deep Ultra-Violet Measurements of SiON Anti-Reflective Coating by Spectroscopic Ellipsometry", Thin Solid Film 313-314, 742 (1998)
4. E.K. Pavelchek, M. deCanto, "A Tunable AR for DUV Lithography", Proc. SPIE **3049**, 932 (1997)
5. D. J. Guerrero, J. D. Meador, G. Xu, H. Suzuki, Y. Sone, V. Krishnamurthy, J. Claypool, J.E. Lamb III, "Deep Ultraviolet Antireflective Coating with Improved Conformality, Optical Density, and Etch Rate", Proc. SPIE **3333**, 228 (1998)
6. T. Ogawa, H. Nakano, T. Gocho, T. Tsumori, "SiO_xN_y:H, high performance anti-reflective layer for the current and future optical lithography", Proc. SPIE **2197**, 722 (1994)
7. T. Gocho, T. Ogawa, M. Muroyama, J. Sato, "Chemical Vapor Deposition of Anti-Reflective Layer Film for Excimer Laser Lithography", Jpn. J. Appl. Phys. **33**, 486 (1994)
8. C.H. Hsiao, C.C. Hsu, "A Novel Inorganic SiON PECVD Anti-Reflective Layer (PE ARL) for Sub-half Micro Optical Lithography", Proc. DUMIC 1998, 327
9. G. Y. Lee, Z. G. Lu, D. M. Dobuzinsky, X. J. Ning, G. Costrini, "Dielectric Anti-Reflection Coating Application in a 0.175 μm Dual-Damascene Process", Proc. IITC 98, 87